4 Electronic Structure of Condensed Matter

4-1 High-Throughput Characterization of the Surface Electronic Structure of Strongly-Correlated Transition Metal Oxide Thin Films Using *in-situ* Photoemission Spectroscopy

Perovskite transition-metal oxide thin-films and superlattices attract much attention not only for their basic scientific interest but also for their technological applications, such as tunneling junction devices. Extensive studies of perovskite oxides films have demonstrated that the magnetic and electronic properties of the oxides can be controlled through interface effects such as spin exchange, charge transfer, and epitaxial strain. The lack of information about the interface and surface electronic structures, however, presents us from fabricating tailored thin films with the properties which we desire. In order to investigate the surface and interface electronic structures of transition metal oxide thin films, we have constructed a system which combines a high-resolution photoemission spectroscopy (HR-PES) system with a combinatorial laser molecular-beam epitaxy (laser MBE) thin film growth system at BL-1C. Figure 1 shows a schematic view of the constructed "*in situ* HR–PES-laser MBE system". The distinctive feature of this system is the direct connection from the spectrometer to the combinatorial laser MBE chamber; thin film samples can be transferred quickly into the photoemission chamber without breaking the ultra-high vacuum. The combinatorial laser MBE system can be used for fabricating combinatorial thin film libraries, i.e. by using physical masking during deposition to grow films under different deposition conditions with different compositions or with different thicknesses at different places of a single substrate. Mapping electronic structures can be performed in a single growth-characterization cycle by scanning the position of the synchrotron radiation beam. The capabilities of the system are demonstrated in Fig. 2, where we have characterized by *in-situ* photoemission the electronic structure of a terminating-layer-controlled $La_{0.6}Sr_{0.4}MnO_3$ (LSMO) thin-film library (left panel of Fig. 2) fabricated on wet-etched TiO_2-terminated $SrTiO_3$(001) (STO) substrates. By plotting the Sr 3d core level intensity as a function of the kinetic energy and of the synchrotron-radiation beam position on this library (middle panel of Fig. 2), we immediately notice significant differences in the surface electronic structures of different parts of the library. Detailed analysis of the Sr 3d core-level line shape shown in the right hand panel of Fig. 2 reveals that the considerable difference in the chemical bonding states of the Sr atoms in the surface regions stems from the difference in terminating layer of each film; for LSMO/SrO/STO (SrO/STO) the dominant terminating layer is La/SrO (SrO), while for LSMO/STO (STO) the MnO_2 (TiO_2) layer dominates. These results show that the terminating layer of the LSMO films can be changed from an MnO_2 to an La/SrO layer by inserting one atomic layer of SrO between the LSMO film and a TiO_2-terminated STO substrate.

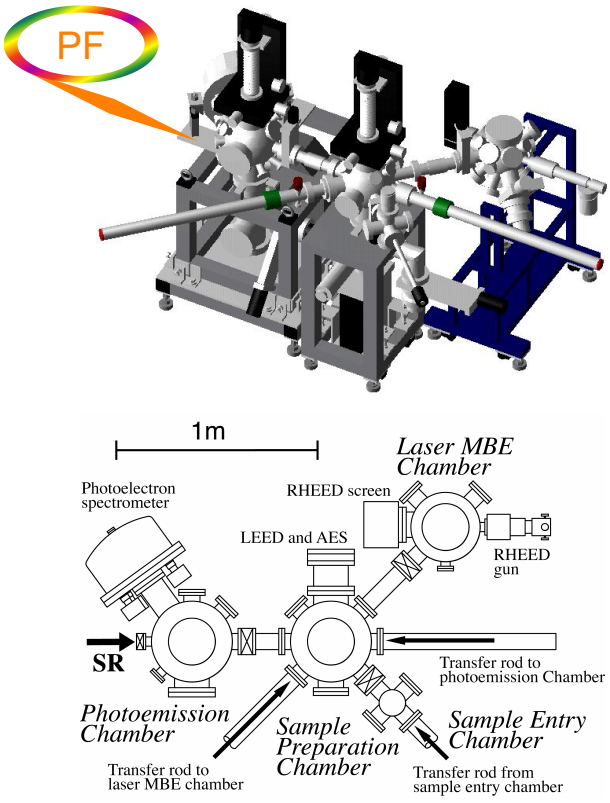

Figure 1
A schematic bird's eye view (top) and a layout diagram (bottom) of the "*in situ* HR-PES-laser MBE system".

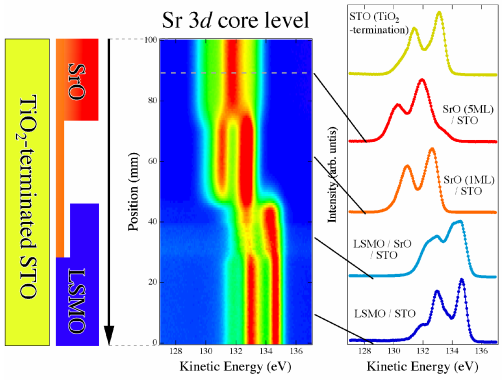

Figure 2
Cross-sectional schematics for the combinatorial library (left), Sr 3d core level imaging for the library (middle), and high-resolution Sr 3d core level spectra (right) .

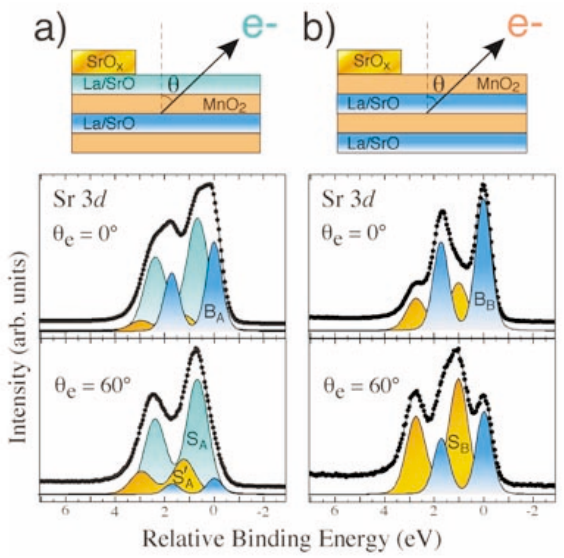

Figure 3
Sr 3d core-level spectra and their decompositions for (a) LSMO/SrO/STO and (b) LSMO/STO at emission angles 0°, 45°, and 60°. Each component is indicated by different colors.

More detailed information on these Sr 3d spectra can be obtained by curve fitting, as shown in Fig. 3. It is clear that the Sr 3d core level consists of three components labeled B_A, S_A, and S'_A for LSMO/SrO/STO while only two major components, B_B and S_B, are visible in the spectra of LSMO/STO. The reduced intensities of the B_A and B_B components under surface-sensitive conditions (θ = 60°) indicate that these components originate from the Sr atoms in an La/SrO layer below an MnO_2 plane. In contrast, the opposite angular behavior of the other components (S_A, S'_A, and S_B) indicates their surface origin. By taking into account the different terminating layers of the two LSMO films, we can assign the second doublet S_A with the chemical shift (CS) values of 0.68±0.01 eV in LSMO/SrO/STO to Sr atoms in the uppermost La/SrO layer. On the other hand, in LSMO/STO, the surface component of S_B is attributed to the presence of Sr atoms on the MnO_2 terminating layer. The Sr atoms remaining at the MnO_2-topmost layer may result in either a local La/SrO-terminated surface or in other crystal phases. The considerable difference in the CS values between the S_A (0.68±0.01 eV) and S_B (1.02±0.02 eV) components indicates that the Sr atoms on the MnO_2-terminated surface have different chemical bonding-states to the Sr atoms in the La/SrO terminated surface. From the viewpoint of magnetic tunneling junctions where tunnelling occurs at the surface boundary, the accumulation and possible recrystallization of Sr at the surface may seriously affect the electronic and magnetic properties of a superlattice made of these perovskite oxides.

H. Kumigashira[1], K. Horiba[1], H. Ohguchi[1], D.Kobayashi[1], M. Oshima[1], N. Nakagawa[1], T. Ohnishi[1], M. Lippmaa[1], K. Ono[2], M. Kawasaki[3] and H. Koinuma[4] ([1]Univ. of Tokyo, [2]KEK-PF, [3]Tohoku Univ., [4]Tokyo Inst. of Tech.)

4-2 Extraction of a Replicative Multi-Electron Contribution to XANES Spectra by Comparative Soft X-Ray Absorption and Emission Spectroscopy

X-ray absorption spectroscopy, especially in the near edge region, is one of the most powerful methods available for probing the unoccupied part of the electronic structure of materials and has been widely used for many applications [1]. Absorption spectra, however, are overlaid with contributions from multielectron transitions because of the definite shake probability for the promotion of valence electrons when the exciting photon energy reaches the onset for multiple excitations. Although this onset energy can be calculated by the Z+1 approximation [2], it is difficult to estimate quantitatively the ratio between the contributions of single- and multiple-excitation in the absorption spectrum above the threshold for multi-electron excitation.

With the advent of recent synchrotron radiation sources, a detailed study of multielectron excitation processes, *e.g.* shake-up single ionization and shake-off double ionization accompanying inner-shell photoionization, in the near threshold region has become possible to investigate intra-atomic electron-electron correlations [3]. In such experiments, the intensities of X-ray satellite or hypersatellite lines arising from core-to-core transitions are measured as a function of the exciting photon energy by X-ray emission spectroscopy (XES). In the present study,

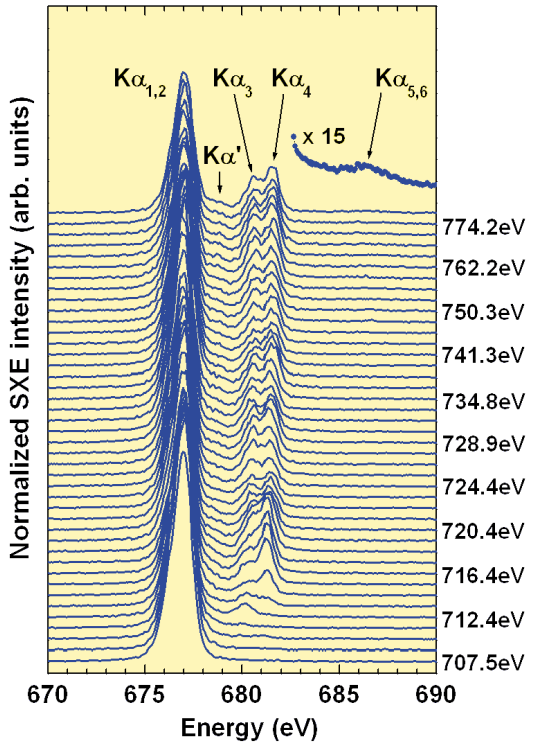

Figure 4
Spectral variation of the F Kα emission for NaF. Typical energies of the exciting photons are shown beside each spectrum.

we have applied this technique to an F-K fluorescence XANES measurement which involves the valence-to-core transitions, and succeeded in determining quantitatively the contribution of multielectron excitation processes to the XANES spectrum [4].

The experiments were performed at BL-2C undulator station. The sample used was an ionic fluorine compound of NaF, which is a stable ionic insulator crystal forming in the NaCl structure. The fluorine Kα spectrum was measured using a soft X-ray emission (SXE) spectrometer and the F-K absorption spectrum was also measured by means of the total photon yield (TPY) method using a photodiode. Figure 4 shows the spectral variation of the F Kα emission for NaF as a function of excitation energy. In addition to the $K\alpha_{1,2}$ diagram lines at 677 eV, $K\alpha_{3,4}$ satellite lines were observed to appear near the onset of [1s2p] double excitation, where the square brackets indicate hole states. The onset can be calculated to be about 706.7 eV, and the spectral shape was found to be very sensitive to the excitation energy. The peak intensities of these lines were carefully determined by means of a least-squares fitting procedure and all the results were normalized to the accumulation time and incident photon flux. In Fig. 5, the normalized intensities are plotted as a function of the incident photon energy together with the F-K XANES spectrum for comparison.

As can be seen in Fig. 5, the energy dependence of the total SXE yield (blue circles), given by $K\alpha_{1,2}$ + $K\alpha L^1$ + $K\alpha L^2$ where $K\alpha L^n$ denotes a configuration with a single K vacancy and nL vacancies, looks very similar to the absorption spectrum. Thus it is apparent that the red circles give the F-K absorption spectrum free from the contribution of multielectron transitions, while the curve of the $K\alpha L^1$ yields (blue triangles) represents the excitation function of [1s2p] double excitation. This curve shows the double excitation of 1s and 2p electrons into the F 3p states forming the unoccupied t_{1u} molecular orbital,

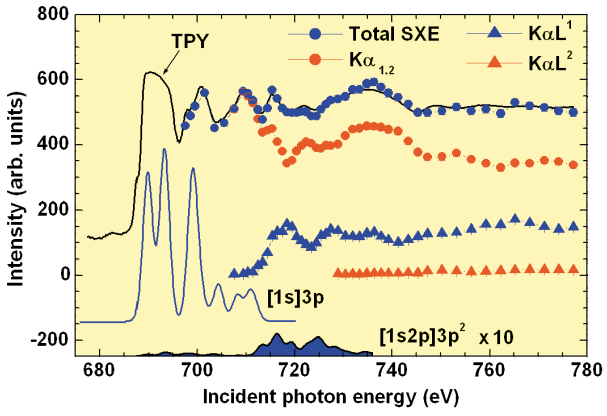

Figure 5
The F-K absorption spectrum (upper solid line) of NaF measured by the TPY method. The normalized SXE yields are plotted as a function of the exciting photon energy for comparison. Theoretical fluorescence XANES spectra for the [1s]3p single excitation (lower solid line) and the [1s2p]$3p^2$ double excitation (solid line with shade) are also presented.

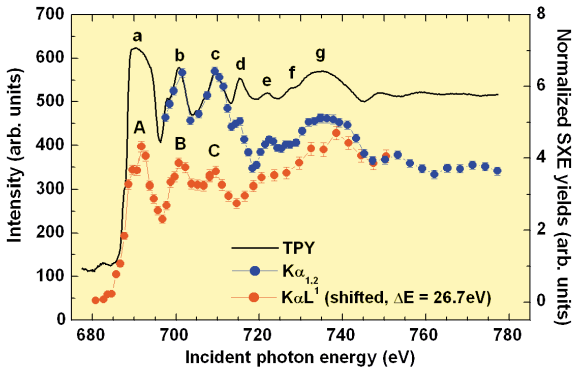

Figure 6
The F-K absorption spectrum (thick solid line) of NaF compared with the evolution curves for the normalized SXE yields for the $K\alpha_{1,2}$ and $K\alpha L^1$ lines. The $K\alpha L^1$ satellite intensity's evolution is shifted along the energy axis by 26.7 eV to the lower energy side.

namely the [1s2p]$3p^2$ state, as confirmed by theoretical calculations.

Furthermore, if we plot the energy-shifted $K\alpha L^1$ satellite intensity's evolution with ΔE = 26.7 eV to the lower energy side, we can find a close resemblance between the energy-shifted $K\alpha L^1$ curve and the F-K absorption spectrum as shown in Fig. 6. This energy shift ΔE = 26.7 eV is in fairly good agreement with theoretical energy difference 23.6 eV between the [1s]3p single excitation and the [1s2p]$3p^2$ double excitation. This would imply that the excitation function for the [1s2p] double excitation, although it locates at higher energy side due to existence of a 2p spectator hole, represents the replicative excitation function reflecting that for single excitation. Such a phenomenon was predicted by Brown *et al*. more than 30 years ago and the present study might demonstrate the evidence for their prediction.

The present results have elucidated that the structure observed above 710 eV in the F-K XANES spectrum of NaF does contain the contribution of multielectron transitions and it can be separated into each component by observing the satellite intensity's evolution with fine energy steps. This method should be applicable for all kinds of materials and give further insight into understanding absorption spectrum in XANES region.

M. Oura[1], T. Mukoyama[2], M. Taguchi[1], T. Takeuchi[1,3] and S. Shin[1,4] ([1]RIKEN/SPring-8, [2]Kansai Gaidai Univ., [3]Tokyo Univ. of Sci., [4]Univ. of Tokyo)

References

[1] F. de Groot, *Chem. Rev.* **101** (2001) 1779.
[2] M. Deutsch, *Phys. Rev. A* **39** (1989) 3956.
[3] M. Oura, H. Yamaoka, K. Kawatsura, K. Takahiro, N. Takeshima, Y. Zou, R. Hutton, S. Ito, Y. Awaya, M. Terasawa, T. Sekioka and T. Mukoyama, *J. Phys. B* **35** (2002) 3847, and references therein.
[4] M. Oura, T. Mukoyama, M. Taguchi, T. Takeuchi, T. Haruna and S. Shin, *Phys. Rev. Lett.* **90** (2003) 173002.
[5] F. C. Brown, C. Gähwiller, H. Fujita, A.B. Kunz, W. Scheifley and N. Carrera, *Phys. Rev. B* **2** (1970) 2126; S.T. Pantelides and F.C. Brown, *Phys. Rev. Lett.* **29** (1974) 298.

4-3 Half-Metallic Density of States in Sr_2FeMoO_6 Observed by Photoemission Spectroscopy

Colossal magnetoresistance (CMR) phenomena have been stimulating a large amount of research on the manganese oxides due to their potential applications to magneto-transport devices [1]. For industrial applications, however, one of the necessary properties is to work in a low magnetic field at room temperature (RT), and hence tunneling magnetoresistance (TMR) phenomena have been getting more attention. To realize such properties, the electronic structure should ideally have a half-metallic density of states (DOS) with a high Curie temperature (T_c). Although the CMR manganites are usually half-metallic [2], many of them have a low T_c and need a high magnetic field. Recently, Kobayashi *et al.* have reported that a double perovskite (DP) Sr_2FeMoO_6 showed a large TMR at RT and also predicted a half-metallic DOS [3]. In spite of the apparent similarity of the near-E_F DOS, there are several differences, such as ferrimagnetism between Fe and Mo and a high ferrimagnetic T_c. Hence, whether the origin of TMR in DP is the same as in the manganites is still unclear.

To understand the origin of TMR in Sr_2FeMoO_6, we have investigated its electronic structure using photoemission spectroscopy [4]. Single crystals of Sr_2FeMoO_6 were grown by the floating-zone method [5], and the experiments were performed at BL-11D. The total energy resolution was about 50-90 meV FWHM with 65-200 eV photon energies. The chamber pressure was typically 2 $\times 10^{-10}$ Torr and the temperature used was about 20 K. Clean surfaces were obtained by fracturing samples *in situ* at 20 K.

Figure 7 shows near-E_F photoemission spectra taken with several different photon energies $h\nu$. The double peak structures *A* and *B* correspond to the Fe $e_{g\uparrow}$ and the Fe+Mo $t_{2g\downarrow}$ bands predicted by band theory [4]. However, it is not clear at this stage whether the actual DOS is half-metallic or not because the predicted Fe $e_{g\uparrow}$ band is very close to E_F in some calculations [3]. The behaviors of the spectral weights of *A* and *B* are quite different to each other. The inset shows the peak area of *A* and *B* plotted against photon energy $h\nu$. One can see that the spectral weight of *A* (red line) has a minimum at ~80 eV while such a clear minimum is not observed in *B* (blue line). At 80 eV and 90 eV, both the spectral weight and also the line shapes of *B* are almost identical. The photoionization cross section of the Mo 4d orbital has a minimum (the Cooper minimum) near ~80-90 eV [6]. Hence, the minimum of *A* in the inset can be interpreted as the Cooper minimum of the Mo 4d states. This clearly demonstrates that *A* has a contribution from the Mo 4d states whereas *B* has only an undetectably small contribution. This is in perfect agreement with the prediction of band theories. It is, therefore, experimentally confirmed that the Fe

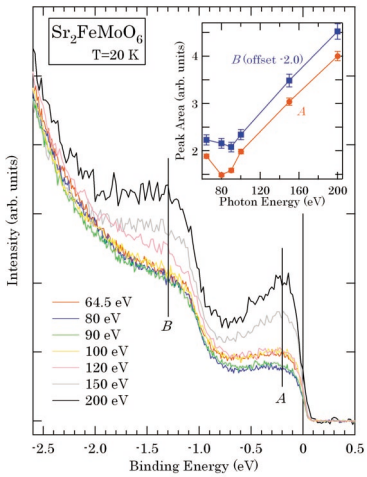

Figure 7
Photoemission spectra of Sr_2FeMoO_6 near the E_F region at T = 20 K taken with several photon energies. Inset: Integrated intensities of peak *A* (at –0.20 eV) and *B* (at –1.30 eV) in 0.1 eV windows plotted as a function of photon energy. Note that the curve for *B* has been offset by –2.0 to enable comparison with the curve for *A* on the same y scale.

$e_{g\uparrow}$ band and the Fe+Mo $t_{2g\downarrow}$ band are distributed from –2.2 eV to –0.9 eV and from –0.9 eV to E_F, respectively, and that only the down-spin band crosses E_F, and is half-metallic.

The double-peak electronic structure is characteristic of Sr_2FeMoO_6 and is a key to understanding the half-metallic DOS of this compound. In the CMR manganites, the charge carriers in the Mn $e_{g\uparrow}$ band are ferromagnetically coupled with the localized Mn $t_{2g\uparrow}$ electrons. For Sr_2FeMoO_6, the double exchange scheme "charge carriers + local spins" is still the same. However, since the Fe up-spin band is completely occupied, the charge carriers are antiferromagnetically coupled with the local spins. Moreover, the up-spin band is pulled down well below E_F due to the strongest ($3d^5$ configuration) Hund's rule coupling at the Fe sites, resulting in the double-peak structure and a half-metallic DOS. Also, a higher T_c would result from the largest local spin (S = 5/2) compared with S = 3/2 for the manganites. Thus, it is concluded that the unique properties of Sr_2FeMoO_6 can be explained by the strong Hund's rule coupling of the $3d^5$ configuration.

T. Saitoh[1], M. Nakatake[2], A. Kakizaki[3], H. Nakajima[4], O. Morimoto[5], Sh. Xu[6], Y. Moritomo[6], N. Hamada[1] and Y. Aiura[7] ([1]Tokyo Univ. of Sci., [2]Hiroshima Univ., [3]Univ. of Tokyo, [4]Natl. Syn. Res. Center, [5]Graduate Univ. for Adv. Studies, [6]Nagoya Univ., [7]Natl. Inst. of Adv. Indust. Sci. and Tech.)

References

[1] For reviews, see C. N. R. Rao and B. Raveau eds., *Colossal Magnetoresistance, Charge Ordering and Related Properties of Manganese Oxides* (World Scientific, Singapore, 1998); Y. Tokura ed, *Colossal Magnetoresistive Oxides* (Gordon and Breach, New York, 2000).
[2] J.-H. Park *et al.*, *Nature* (London) **392** (1998) 794.
[3] K.-I. Kobayashi *et al.*, *Nature* **395** (1998) 677.
[4] T. Saitoh *et al.*, *Phys. Rev. B* **66** (2002) 035112.
[5] Y. Moritomo *et al.*, *Phys. Rev. B* **61** (2000) R7827.
[6] J.J. Yeh and I. Lindau, *At. Data Nucl. Data Tables* **32** (1985) 1.